International Journal of Nanomedicine

Dovepress
open access to scientific and medical research

Open Access Full Text Article

ORIGINAL RESEARCH

Fabrication of Photo-Crosslinkable Poly (Trimethylene Carbonate)/Polycaprolactone Nanofibrous Scaffolds for Tendon Regeneration

This article was published in the following Dove Press journal:
International Journal of Nanomedicine

Xing Li[1,2,*]
Honglin Chen[3,*]
Shuting Xie[1,2]
Ning Wang[3]
Sujuan Wu[1,2]
Yuyou Duan[3]
Minmin Zhang[4]
Lingling Shui[1,2,4]

[1]National Center for International Research on Green Optoelectronics, South China Normal University, Guangzhou 510006, People's Republic of China; [2]Guangdong Provincial Key Laboratory of Optical Information Materials and Technology, South China Academy of Advanced Optoelectronics, South China Normal University, Guangzhou 510006, People's Republic of China; [3]Institute for Life Science, School of Medicine, South China University of Technology, Guangzhou 510006, People's Republic of China; [4]School of Information and Optoelectronic Science and Engineering, South China Normal University, Guangzhou 510006, People's Republic of China

*These authors contributed equally to this work

Correspondence: Minmin Zhang; Lingling Shui
Tel +86-20-39310508; +86-20-39310309;
Email zhangminmin@m.scnu.edu.cn; shuill@m.scnu.edu.cn

Background: The treatment of tendon injuries remains a challenging problem in clinical due to their slow and insufficient natural healing process. Scaffold-based tissue engineering provides a promising strategy to facilitate tendon healing and regeneration. However, many tissue engineering scaffolds have failed due to their poor and unstable mechanical properties. To address this, we fabricated nanofibrous polycaprolactone/methacrylated poly(trimethylene carbonate) (PCL/PTMC-MA) composite scaffolds via electrospinning.

Materials and Methods: PTMC-MA was characterized by nuclear magnetic resonance. Fiber morphology of composite scaffolds was evaluated using scanning electron microscopy. The monotonic tensile test was performed for determining the mechanical properties of composite scaffolds. Cell viability and collagen deposition were assessed via PrestoBlue assay and enzyme-linked immunosorbent assay, respectively.

Results: These PCL/PTMC-MA composite scaffolds had an increase in mechanical properties as PTMC-MA content increase. After photo-crosslinking, they showed further enhanced mechanical properties including creep resistance, which was superior to pure PCL scaffolds. It is worth noting that photo-crosslinked PCL/PTMC-MA (1:3) composite scaffolds had a Young's modulus of 31.13 ± 1.30 MPa and Max stress at break of 23.80 ± 3.44 MPa that were comparable with the mechanical properties of native tendon (Young's modulus 20–1200 MPa, max stress at break 5–100 MPa). In addition, biological experiments demonstrated that PCL/PTMC-MA composite scaffolds were biocompatible for cell adhesion, proliferation, and differentiation.

Keywords: poly(trimethylene carbonate), composite scaffolds, tissue engineering, photo-crosslinking, creep resistance

Introduction

Tendon injuries are frequently-occurring diseases in our daily life. It was estimated that over 25% of adults have suffered a tendon-related musculoskeletal problem.[1] In case of severe tendon injuries, their natural healing processes are slow and insufficient due to the low innervation, hypovascularity, and hypocellularity of these tissues.[2,3] Surgical intervention is the main reconstruction strategy, including autografts, allografts, and xenografts.[4,5] However, the clinical outcomes of tendon repair remain unsatisfactory as a result of the limit of grafts' donor source, the existence of immune rejection and inflammation.[6]

Tissue engineering, also known as"regenerative medicine", is an interdisciplinary field which combines life sciences, materials science, and engineering towards

the development of biological substitutes that restore, maintain, or replace diseased tissues.[7] Scaffold-based tissue engineering which is the use of a combination of cells, scaffolds and growth factors to develop functional replacements for traditional grafts, shows great potential for application in the clinical treatment of tendon injuries.[6,8,9] Currently, techniques for fabricating tissue engineering scaffolds mainly include 3D printing,[10] knitting machine,[11] and electrospinning.[12] Electrospinning is a versatile and simple approach for generating nanofibrous scaffolds that mimic the structure of native extracellular matrix.[13,14] As such, electrospinning has been widely used for fabricating tissue engineering scaffolds.

How to improve mechanical properties of electrospun scaffolds is one of the most important aspects in tissue engineering.[1,6,15,16] In general, there are three methods to improve the mechanical properties of electrospun scaffolds including design specific structure for scaffolds, composite scaffolds with other materials and photo-crosslinking. The process of constructing specific structure is complicated.[17] While it is simple and common to improve the mechanical properties of polymer scaffolds by physically mixing them with other materials to form composite scaffolds and via photo-crosslinking.[18] Forming a polymer network by chemically crosslinked polymers is beneficial to improve creep resistance of scaffolds.[19] For example, Chen et al used a photo-crosslinkable polymer, polylactic acid-co-acrylate, to prepare an electrospun-oriented fiber scaffold. Cyclic tensile test results showed that photo-crosslinked scaffold has good creep resistance.[20]

Polycaprolactone (PCL) is an aliphatic linear polyester which has been approved by the FDA for clinical application due to its biocompatibility, bioabsorbability and low cost.[21] However, PCL exhibits a low degradation rate due to its semi-crystalline and hydrophobic nature resulting in a relatively slow healing process of injured tendons.[22–24] Besides, poor mechanical tolerance of PCL is another drawback for its further application in clinical.[25]

Poly(trimethylene carbonate) (PTMC), another FDA approved material, is a rubber-like polymer with a glass transition temperature (Tg) around −20°C.[19,21] PTMC has unique degradation behaviors such as enzymatic degradation with a surface erosion process, without formation of acidic products, and resistance to non-enzymatic hydrolysis.[26,27] Therefore, this elastomeric polymer has been exploited in regenerative medicine, including vascular tissue engineering,[28,29] bone defect repair,[30,31] and drug loading implantation.[32,33] To the best of our knowledge, the use of PTMC in tendon regeneration have not been investigated. It is worth noting that PTMC is soft with a poor rigidity.[23,28] Thus, fabrication of PTMC nanofibrous scaffolds by electrospinning remains a challenge since PTMC fibers will collapse and fuse together.[33–35]

In the present work, photo-crosslinkable PTMC (PTMC-MA) macromers were prepared by ring-opening polymerization of 1,3-Dioxane-2-one (TMC) monomers and subsequently functionalized with methacrylate. PTMC-based nanofibrous scaffolds were prepared by electrospinning of mixed solutions of PCL and PTMC-MA. Our hypothesis was that the introduction of PCL would facilitate PTMC-MA electrospinning. Furthermore, it was expected that the use of photo-crosslinkable PTMC-MA instead of PTMC would enhance the creep resistance of composite scaffolds. The properties of PCL/PTMC-MA composite scaffolds, including fiber morphology, fiber orientation, and mechanical properties were investigated. To determine the cellular compatibility of PCL/PTMC-MA composite scaffolds for their potential applications in tendon tissue engineering, mouse mesenchymal stem cells were cultured on the scaffolds, and their cell proliferation and differentiation were evaluated later on.

Materials and Methods

Materials

1,3-Dioxane-2-one (trimethylene carbonate, TMC) was obtained from Jinan Daigang Biomaterial Co., Ltd. (Jinan, China). Polycaprolactone (PCL, Mn≈80 kg/mol), 1,1,1-tris(hydroxymethyl) propane (trimethylolpropane, TMP), Tin (II) ethylhexanoate ($Sn(Oct)_2$), methacrylic anhydride (94%, MMAh), triethylamine (TEA), ascorbic acid (AA) and deuterated chloroform were all purchased from Sigma-Aldrich (MO, USA). Calcium hydride and Irgacure 2959 (2-hydroxy-4-(2-hydroxyethoxy)-2-methylpropiophenone, D2959) were purchased from Aladdin Inc. (Shanghai, China). Dichloromethane (DCM), methanol, and dimethylformamide (DMF) were received from Tianjin Zhiyuan Chemical Reagent Factory (Tianjin, China). DCM was dried by calcium hydride and distilled under N_2 atmosphere before use. Hydroquinone was purchased from Tianjin Damao Chemical Reagent Factory (Tianjin, China). High-glucose Dulbecco's Modified Eagle's Medium (DMEM) and Fetal bovine serum (FBS) were supplied from Biological Industries (Israel), Trypsin and Penicillin-Streptomycin-Gentamicin Solution were purchased from Solarbio Inc. (Beijing, China).

PrestoBlue™ HS Cell Viability Reagent was purchased from Thermo Fisher Scientific (Massachusetts, USA). Mouse collagen type I ELISA kit was purchased from Qchen Bio Co., Ltd. (Shanghai, China). All other reagents and organic solvents are of analytic reagent (AR) without further treatment prior to use.

Synthesis of Methacrylated Poly (Trimethylene Carbonate)

Three-armed PTMC was prepared by ring-opening polymerization (ROP) of TMC initiated by TMP as previously described.[36] PTMC's molecular weight was controlled by varying the amount of TMP. Briefly, TMC/TMP, in a molar ratio of 500/1, was loaded in a dry eggplant-shaped flask under dry N_2 atmosphere. The polymerization was carried out at 130°C for 3 days using 0.13 wt% of $Sn(Oct)_2$ as a catalyst. The resulting polymer was purified by dissolving in dry DCM and followed by precipitating in cold methanol for 3 times. The precipitate was dried at room temperature in vacuo. In order to obtain a photo-crosslinkable compound, PTMC-MA was subsequently synthesized using an established protocol with slight modification.[37] Three-armed PTMC was functionalized in DCM (5 mL/g, PTMC) by reaction with MAAh (4 mol/mol) in the presence of TEA (4 mol/mol) and hydroquinone (0.03 mol/mol). The functionalized reaction was conducted at room temperature for 5 days avoiding light. Reacted PTMC-MA solution was extracted with demineralized water 3 times and the organic phase was precipitated in cold methanol. The precipitate was firstly dried in the dark at ambient conditions overnight and then further dried in vacuo at room temperature until its weight kept constant.

Both PTMC and PTMC-MA were characterized by nuclear magnetic resonance (NMR) spectroscopy (Mercury-plus 300, Varian, USA) and gel permeation chromatography (GPC, Waters Breeze, Waters, USA; eluent: tetrahydrofuran; flow rate: 1.0 mL per minute; column calibration: polystyrene standards). The degree of functionalization of PTMC-MA was determined by ^{1}H NMR, and deuterated chloroform was used as a solvent. The average-number molecular weight and molar-mass dispersity were measured using GPC.

Fabrication of Photo-Crosslinked Scaffolds with Aligned Orientation

Polymer solution (10%, w/v) was prepared by dissolving PCL and PTMC-MA in DCM/DMF (v/v = 3:1) with different weight ratios of PTMC-MA to PCL. The resultant mixtures were stirred for 12 h to obtain homogenous solutions before electrospinning. For electrospinning, polymer solution was extruded through a 20-gauge blunt-tip needle at a flow rate of 5 mL/h with a distance of 15 cm between spinneret and mandrel. The spinneret was charged with a voltage of 25 kV, and aligned nanofibers were collected using a mandrel at speed of 2000 rpm. Electrospinning was performed at ambient condition (room humidity H_{room} = 30–50% and room temperature T_{room} = 23–28°C).

To obtain photo-crosslinked nanofibers, electrospun scaffolds were immersed in D2959 aqueous solution (1 wt%) for 2 h, followed by exposure to UV light source (0.072 W*cm^{-2}) for 10 min each side. After crosslinking, electrospun scaffolds were gently washed with ethanol and PBS. The final electrospun scaffolds were dried under vacuum at room temperature (T_{room} = 23–28°C) for 12 h.

Characterization of PCL/PTMC-MA Photo-Crosslinked Scaffolds

The morphology of the scaffold was characterized using scanning electron microscope (SEM, Phenom G2 Pro, PhenomWorld, The Netherlands) at 5 kV. Samples were fixed at the stage with electroconductive paste and sputter coated with platinum (≈2 nm, 120 s, 20 mA) before SEM imaging. The average fiber diameter and orientation of scaffold were determined by analyzing at least 500 fibers (n≈120, 5 images per scaffold) from SEM images using ImageJ software.

The monotonic tensile test was performed for determining the mechanical properties of before photocrosslinking and after crosslinking scaffolds. Briefly, each scaffold was cut into 15 mm × 50 mm strips with the same thickness (50~70 μm) before testing. All strips were strained at a rate of 20 mm/min using a pneumatically powered tensile tester (Instron 5697, USA). Moreover, to further confirm the influence of photocrosslinking treatment on mechanical behavior, strips with 50% content PTMC-MA (PCL/PTMC-MA (1:1)) were pulled to 20% strain for 20 cycles, and the change of gauge length was recorded every cycle. All tests were performed in the same external conditions (T_{room} = 20–30°C and H_{room} = 50–60%, n = 3).

Cell Culture and Seeding on Scaffolds

Green fluorescent protein $(GFP)^+$ C57BL/6 mouse mesenchymal stem cells (MSCs) were obtained from Cyagen Biosciences (Guangzhou, China). MSCs were

expanded in T-25 flask, and cultured in a medium, comprised of high-glucose DMEM, 10% (v/v) FBS, 1% (v/v) penicillin-streptomycin-nystatin and 0.01% (v/v) ascorbic acid. Cells were harvested at approximately 80% confluence for further scaffold-based study.

Photo-crosslinked electrospun scaffolds were punched into discs (diameter = 1 cm) and placed inside a 48-well plate (n = 3, for each group). For sterilization, the scaffolds were immersed in 75% ethanol for 45 min for 3 times, followed by washing with PBS 3 times for 15min each to remove remaining ethanol. After that, sterile scaffolds were immersed in the cell culture medium overnight before cell seeding. After removing the medium from scaffolds, MSCs were seeded on each scaffold at a density of 15,000 cells/well in 100 μL cell culture media. Cell-scaffold constructs were incubated for 2 h to allow cell attachment and topped up to 0.5 mL cell culture media. The cell-scaffold constructs were cultured in an incubator with 5% CO_2 humid atmosphere at 37°C for up to 21 days. Cell culture media was refreshed every two days.

Cell Distribution and Viability

The distribution of MSCs on scaffolds was analyzed using an Inverted fluorescence microscope (AX10, ZEISS, German). The viability of cells seeded on scaffolds was analyzed by PrestoBlue™ assay according to the vendor's protocol. Briefly, cell culture media was replaced with a medium containing 10% (v/v) PrestoBlue™ HS reagent, and samples were wrapped with aluminum foil to avoid light, followed by incubating at 37°C for 45 min. Two blank wells added with 500 μL Presto Blue™ HS reagent worked as a control. Fluorescence intensity was measured in a microplate reader (Biotek Cytation 5, USA; Excitation 560 nm/Emission 590 nm). Cell viability was measured at days 1, 4, and 7.

Enzyme-Linked Immunosorbent Assay (ELISA)

The concentration of collagen type I in cell culture medium produced from MSCs was quantified by ELISA. Briefly, the same volume of cell culture medium was collected at time points of days 1, 4, 7, 14 and 21, and preserved at −80°C before further analysis. For collagen type I quantification, samples were assessed using a collagen type I Elisa kit following the vendor's protocol. The absorbance was recorded at 450 nm in a microplate reader (Biotek Cytation 5, USA).

Statistical Analysis

The statistical analysis of data was performed using the GraphPad PRISM version 7.00. Two-way analysis of variance (ANOVA) followed by the Tukey post hoc test for multiple comparisons was performed, unless specified otherwise. The results were presented as mean ± standard deviation, and $p < 0.05$ meant statistical significance.

Results and Discussion

Synthesis of PTMC-MA

In the present work, three-armed PTMC was prepared by ROP of TMC using TMP as an initiator. The product was subsequently functionalized with methacrylic anhydride to yield photo-crosslinked PTMC-MA (Figure 1A). The obtained PTMC macromers had a relatively low molecular weight (Mn = 21.90 kg/mol or M_W = 34.30 kg/mol) and moderate molar-mass dispersity (PDI = 1.56) measured by GPC (Table S1). A relatively low molecular weight would benefit the increase of scaffold's mechanical properties after crosslinking, since the number of methyl propylene functional groups depend on the number of polymers.[19] By comparing the ^{1}H NMR spectra of PTMC-MA with PTMC, the appearance of the double bond proton peaks at 5.57 ppm and 6.11 ppm in PTMC-MA clearly confirmed the end-group functionalization of PTMC with methacrylic anhydride (Figure 1B). The degree of functionalization was determined following a similar method as reported by Geven et al.[36] An average degree of functionalization of approximately 75% could be calculated. To evaluate the crosslink density of PTMC-MA network, gel content was measured at different time points of UV exposure (Table S2). The results demonstrated that gel content of PTMC-MA was the highest up to 99.37% after exposure to UV for 10 min. Gel content slightly decreased as the exposure time increase to 15min, which may be attributed to the degradation of network.[38] Thus, the UV exposure time for PCL/PTMC-MA composite scaffolds was set at 10 min.

Fabrication of PCL/PTMC-MA Photo-Crosslinked Scaffolds

Within the native tendon, spindle-shaped tenocytes are organized in linear arrays aligned with and interspersed between nano collagen fibers.[2] Recent studies have

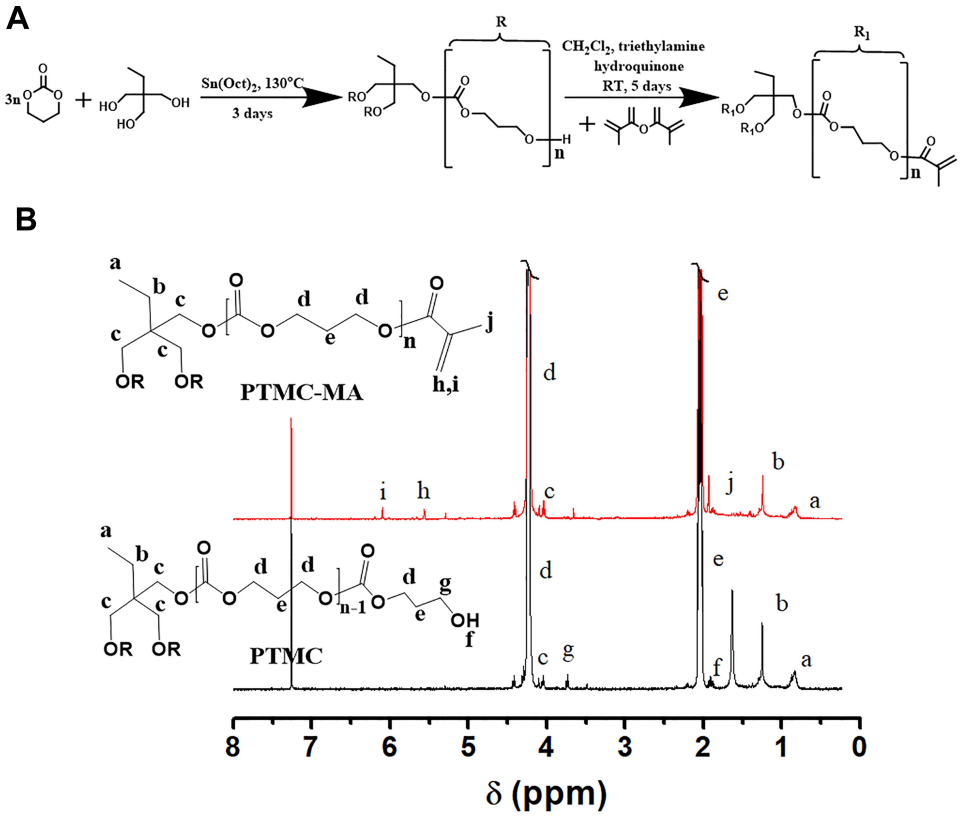

Figure 1 (**A**) The schematic synthesis of the PTMC and its subsequent functionalization using methacrylic anhydride for PTMC-MA. (**B**) Representative ^{1}H NMR spectrum of PTMC and PTMC-MA.

demonstrated that there was a strong relationship between scaffold topography and cell behaviors.[39] For example, the orientation of electrospun fibers has a close connection to the differentiation, elongation, and migration of seed cells.[24,40] Hence, a tissue engineering scaffold should be ideally designed to imitate the microenvironment of ECM, which is beneficial for the treatment of tendon injury. Here, we used electrospinning, a versatile and simple approach, to generate aligned nanofibrous composite scaffolds.

SEM micrographs of composite nanofibers obtained at different mass ratios of PCL to PTMA-MA are shown in Figure 2. The fiber morphology of composite nanofibers was strongly affected by the portion of PTMC-MA. When the portion of PTMC-MA increased from 0% to 50% (pure PCL, PCL/PTMC-MA (3:1), and PCL/PTMC-MA (1:1)), a homogeneous and ultrafine fiber morphology was observed (Figure 2A–C). As the weight ratio reached up to 75% (PCL/PTMC-MA (1:3)), the fibers presented a molten morphology with an increase in fiber interconnection (Figure 2D). No fibrous structure was observed in the fabrication of pure PTMC-MA due to its natural amorphism and poor stiffness resulting in fiber fusing together, especially at relatively lower molecular weight (Figure 2E).[29,33] No significant difference in the morphology of scaffolds before and after immersion in PBS (Figure S1), demonstrating the successful crosslinking of PCL/PTMC-MA composite nanofibers. Figure 2F–H shows the average fiber diameters and diameter distributions of electrospun mats. A similar average fiber diameter (around 600 nm) was detected in spite of an increase of PTMC-MA content from 0% to 50%. The dimension of composite fibers obtained in the present work was comparable to collagen fibers in native tendons.[41] Fiber orientations were analyzed by the statistics of fiber angles in their SEM micrographs (Figure 2I–K). Most PCL fibers were oriented with an angle distribution from −30° to 50°. PCL/PTMC-MA (3:1) fibers (−50° to 50°) had a nearly similar angle distribution range to PCL/PTMC-MA (1:1) fibers (−40° to 50°). However, the latter one presented a more equal distribution at all angles indicating more randomly

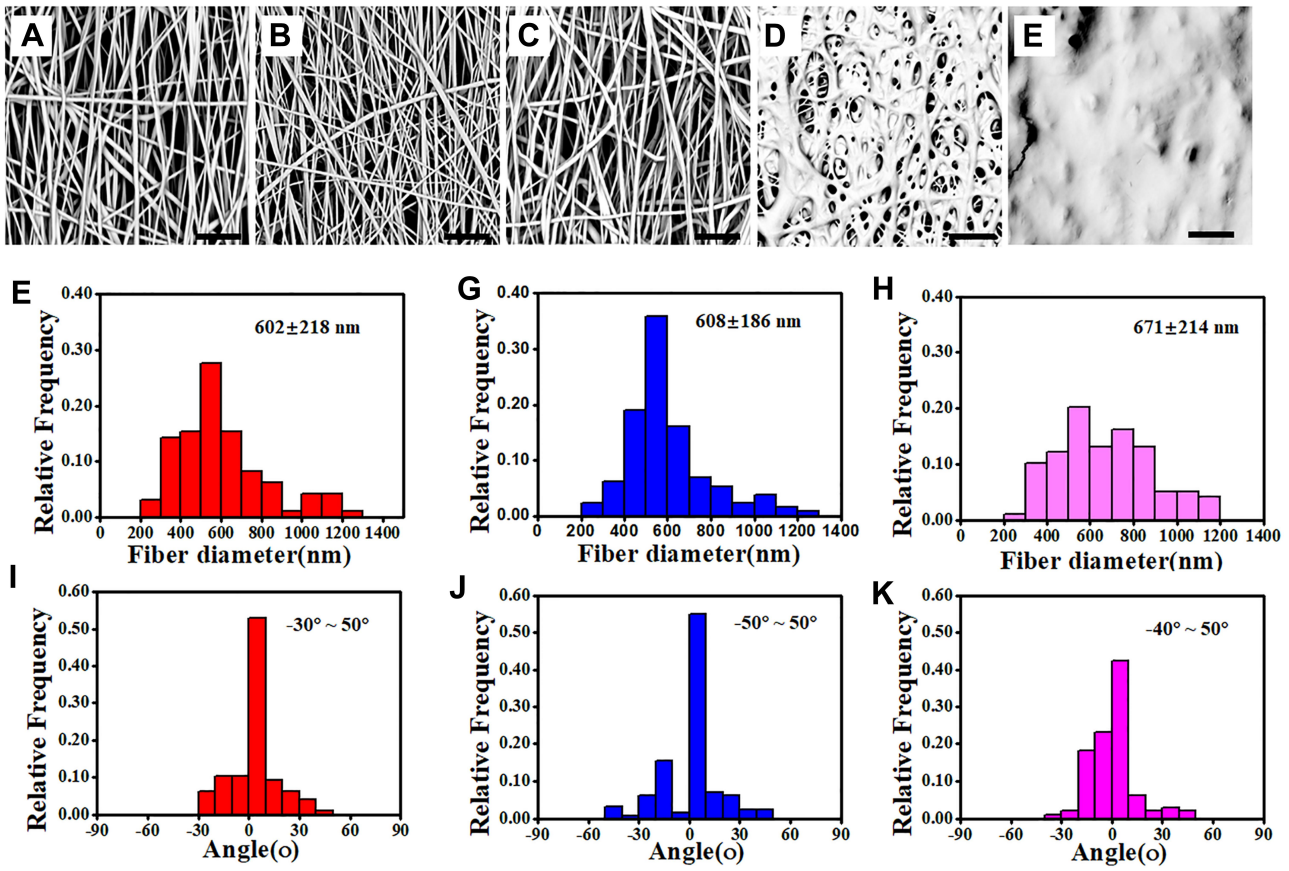

Figure 2 SEM images of electrospun fiber of pure PCL (**A**), PCL/PTMC-MA (3:1) (**B**), PCL/PTMC-MA (1:1) (**C**), PCL/PTMC-MA (1:3) (**D**) and PTMC-MA (**E**). Fiber diameter distributions and fiber orientations of PCL fibers (**F** and **I**), PCL/PTMC-MA (3:1) (**G** and **J**) and PCL/PTMC-MA (1:1) (**H** and **K**). Scale bar: 10 μm.

oriented fibers. Taken together, the increase of three-armed PTMC-MA content would sacrifice the fiber orientation of composite fibers.

Mechanical Properties of PCL/PTMC-MA Photo-Crosslinked Scaffolds

An ideal scaffold should meet a series of mechanical properties for maintaining the basic function after implanting to the body.[42] Mechanical properties of PCL/PTMC-MA composite scaffolds before and after crosslinking were determined by monotonic test (Figure 3). Young's modulus, yield strain, and max stress at break for pure PCL scaffolds were 11.16 ± 0.55 MPa, 77 ± 10%, and 4.96 ± 0.94 MPa, respectively, and these values incrementally increased as the three-armed PTMC-MA content increased. 15.26 ± 2.37 MPa, 126 ± 22%, and 8.35 ± 1.24 MPa for PCL/PTMC-MA(3:1) before crosslinking; 17.00 ± 1.22 MPa, 149 ± 12%, and 10.31 ± 1.82 MPa for PCL/PTMC-MA(1:1) before crosslinking; 19 ± 3.42 MPa, 159 ± 9%, and 13.21 ± 0.47 MPa for PCL/PTMC-MA(1:3) before crosslinking. Previous study has demonstrated that PCL/PTMC composite scaffolds had superior elasticity and stiffness compared with pure PCL scaffolds due to combination of the advantages of PCL and PTMC.[21] The mechanical properties of PCL/PTMC-MA composite scaffolds further enhanced after UV crosslinking, which was reasoned that methyl allyls of functional polyester in UV crosslinked with each other and formed a polymer network.[19] As expected, PCL/PTMC-MA(1:3) composite scaffolds that had the highest PTMC-MA content showed the highest Young's modulus (31.13 ± 1.30 MPa) and max stress at break (23.80 ± 3.44 MPa) after photo-crosslinking. However, the yield strain of photo-crosslinked PCL/PTMC-MA(1:3) scaffolds (170 ± 22%) was lower than that of photo-crosslinked PCL/PTMC-MA (1:1) (190 ± 22%), which may be due to fibers' coagulating.[34]

To investigate the influence of photo-crosslinking on mechanical properties of composite scaffolds, pull-relaxation cycles monotonic test was conducted to evaluate the creep resistance of scaffolds (Figure 4). Creep resistance

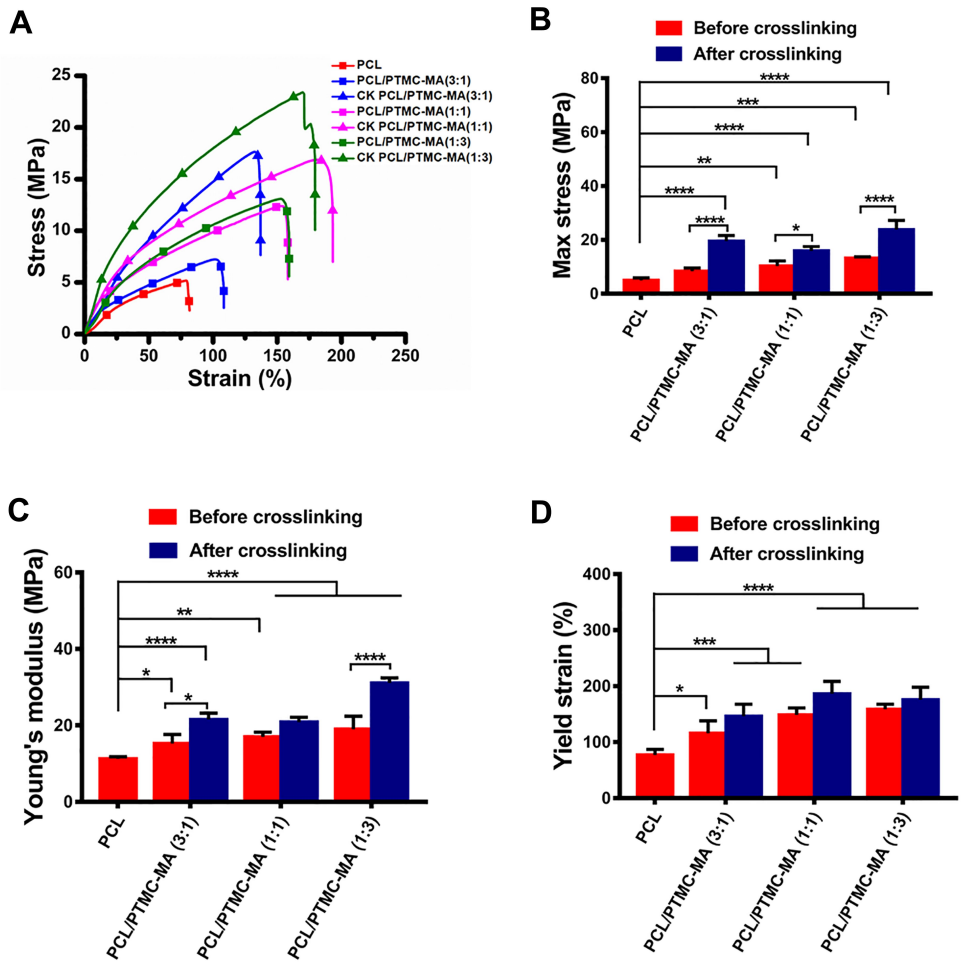

Figure 3 Comparison of tensile mechanical properties of electrospun scaffolds with different PCL/PTMC-MA mass ratios before and after crosslinking. (**A**) Representative stress–strain curves, CK stands for crosslinked. (**B**) Max stress at break. (**C**) Young's modulus. (**D**) Yield strain at break. *p< 0.05, **p< 0.01, ***p< 0.001, and ****p< 0.0001, *p < 0.05 stand for statistical significance.

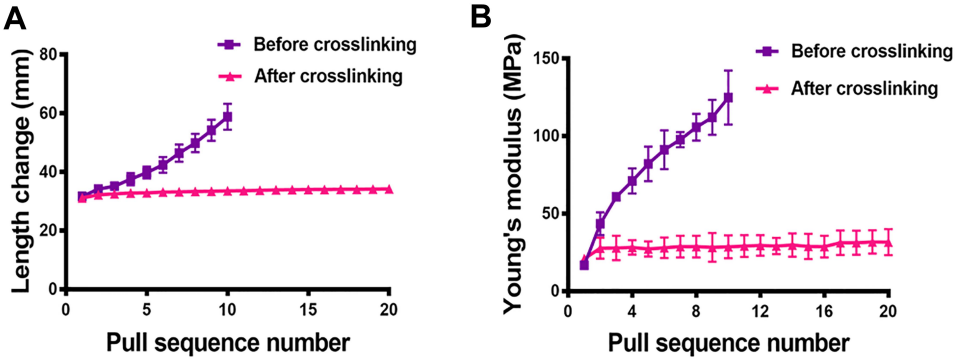

Figure 4 Fatigue test on PCL/PTMC-MA (1:1) before and after crosslinking under 20 times of pull-relaxation cycles. (**A**) Change of sample gauge length, and (**B**) Change of Young's modulus. Scaffolds of PCL/PTMC-MA (1:1) before crosslinking ruptured at the 11th stretch.

is closely related to scaffold stability and plays a key role during tissue regeneration.[6] Each gauge length of the sample was recorded before and after one pull-relaxation monotonic test (Figure 4A). A continuous increase of sample gauge length for non-crosslinked scaffolds was observed during pull-relaxation cycles monotonic tests, and the scaffolds ruptured at the eleventh cycle during the pull-relaxation of non-crosslinked scaffolds. However, the gauge length for crosslinked scaffolds remained almost constant. Note that the Young's modulus for non-crosslinked scaffolds

dramatically increased as the pull sequence cycles increase, which may be caused by the increasing of PCL crystallinity during pulling.[43] In contrast, no obvious difference in Young's modulus for crosslinked scaffolds was observed during pull-relaxation cycles monotonic tests (Figure 4B), indicating more stable scaffolds after photo-crosslinking. Previous studies demonstrated that photo-crosslinked PTMC-MA showed enhanced stability and creep resistance compared with PTMC.[19,28]

Several studies on enhancing mechanical properties of PCL scaffolds have been reported.[44–47] For example, Cheol et al introduced human serum albumin (HSA) to PCL to prepare PCL/HSA composite scaffolds.[48] The mechanical properties of PCL/HSA (Young's modulus 14.39±1.30 MPa; Max stress at break 22.47 ± 3.32 MPa) were higher than those of pure PCL scaffolds (Young's modulus 8.71 ± 0.51 MPa; Max stress at break 5.02 ± 0.41 MPa). Robert et al designed aligned PCL nanofibers to enhance the mechanical properties of PCL scaffold by electrospinning (Young's modulus 9.90 ± 0.87 MPa in PCL aligned compared to 4.02 ± 0.88 MPa in PCL non-aligned).[49] Both mixing with other materials and designing special structures could improve the mechanical properties of PCL scaffolds; nevertheless, the creep resistance of these scaffolds remains no change that limits their applications in tendon tissue engineering. The mechanical properties of our photo-crosslinked PCL/PTMC-MA(1:3) scaffolds show superior mechanical properties to previous reported studies and possess good creep resistance (Table 1). Taken together, photo-crosslinked PCL/PTMC-MA composite scaffolds have comparable mechanical properties to those of native tendon tissue (Young's modulus 20–1200 MPa, max stress at break 5–100 MPa).[50]

Table 1 Comparison of Mechanical Properties of PCL/PTMC-MA Scaffolds with Reported PCL Scaffolds[a]

	Young's Modulus/ MPa	Max Stress at Break/MPa	Reference
Aligned PCL	9.90 ± 0.87	5.20 ± 0.80	[49]
PCL/$NaHCO_3$	32.0 ± 0.59	5.1 ± 2.28	[45]
PCL/HSA[c]	14.39 ± 1.30	22.47 ± 3.32	[48]
PLGA/PCL	7.32 ± 0.21	3.58 ± 0.09	[46]
PCL/NC[b]	32.9 ± 4.4	6.03 ± 0.65	[44]
PCL/Gel-MA	10 ± 1.20	3.80 ± 0.20	[47]
PCL/PTMC-MA	31.13 ± 1.30	23.80 ± 3.44	This paper

Notes: [a]Molecular weight of all PCL is 80 kg/mol. [b]NC represents nanofibrillated chitosan. [c]HSA represents human serum albumin.

Cell Adhesion and Cell Viability

Besides with adequate mechanical properties, an ideal tendon scaffold should be biocompatible after implantation.[4,42] Figure 5 shows fluorescent micrographs of GFP^+ MSCs on PCL/PTMC-MA composite scaffolds with different PTMC-MA content at days 1, 4, and 7 after cell seeding. Generally, cell numbers increased steadily on all scaffolds studied during the time course investigated. Thus, PCL/PTMC-MA composite scaffolds support MSCs adhesion. Previous studies have demonstrated that cells

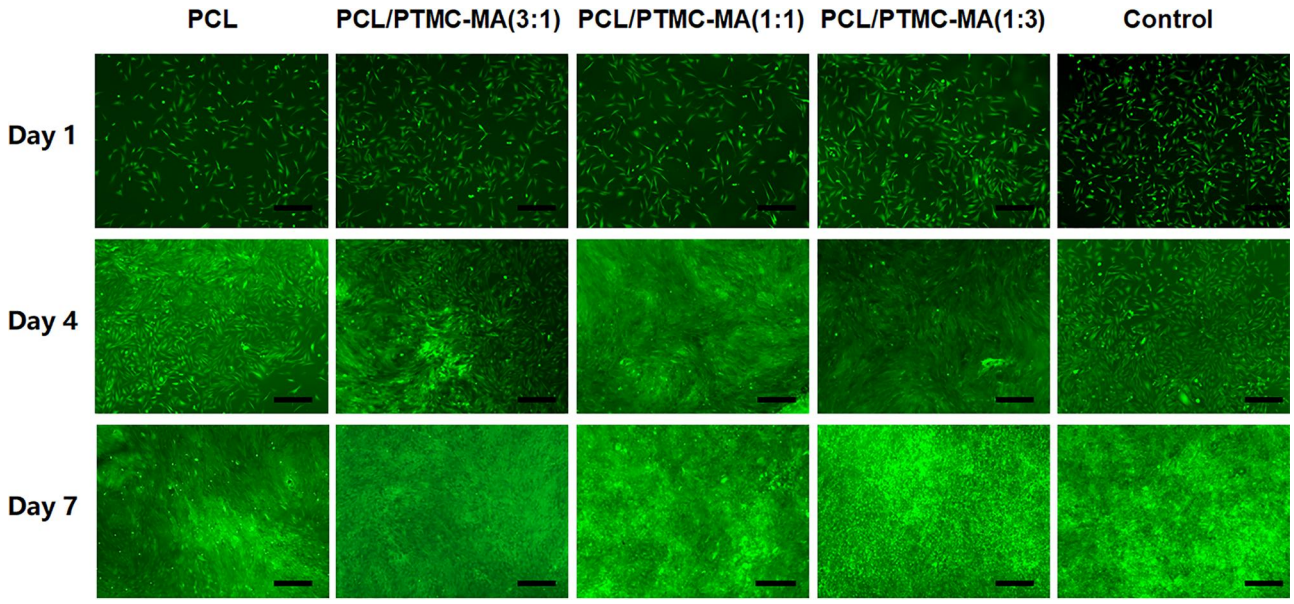

Figure 5 Representative fluorescent micrographs of MSCs density on electrospun scaffolds and tissue culture plates (control) at days 1, 4, and 7. Scale bar: 50 μm.

would grow along the aligned nanofibers.[39,40] In our work, however, due to the properties of PTMC which is soft and elastic, it is difficult to obtain highly aligned PCL/PTMC-MA fibers via a rotating mandrel.

Cell viability is vital for cell growth and proliferation.[51] Cell viability of MSCs on scaffolds was investigated by PrestoBlue™ HS reagent reducing array (Figure 6). Cell viability dramatically increased on all scaffolds from day 1 to day 4 due to the proliferation of MSCs, and it became stable afterward as a result of confluent cell. At day 4, cell viability of MSCs on all electrospun scaffolds was higher than that of tissue culture plate (control), which indicated that electrospun scaffolds were biocompatible and supported MSCs proliferation. PCL/PTMC-MA(3:1) had significantly higher cell viability than PCL/PTMC-MA(1:3) at both day 4 and day 7, which may ascribe to an ultrafine fibrous morphology of PCL/PTMC-MA(3:1) scaffolds leading to a better cell proliferation. For PCL/PTMC-MA(1:3), it is significantly higher than the control plate at day 4. While at day 7, PCL/PTMC-MA(1:3) is lower than the control plate due to cell confluence.

Quantification of Collagen

Type I collagen is the major component of tendon's extracellular matrix (ECM) which is closely related to the osteogenic differentiation of MSCs and important for healing tendon injury.[2,52] To investigate cell differentiation of MSCs on scaffolds, the amount of collagen I was determined by Collagen I ELISA kit (Figure 7). The amount of collagen I on all substrates dramatically increased during the first week and became relatively constant afterward. No significant difference in collagen secretion was observed between composite scaffolds regardless of PTMC-MA content. At days 14 and 21, the amount of collagen I was significantly higher for composite scaffolds than tissue culture plates (control).

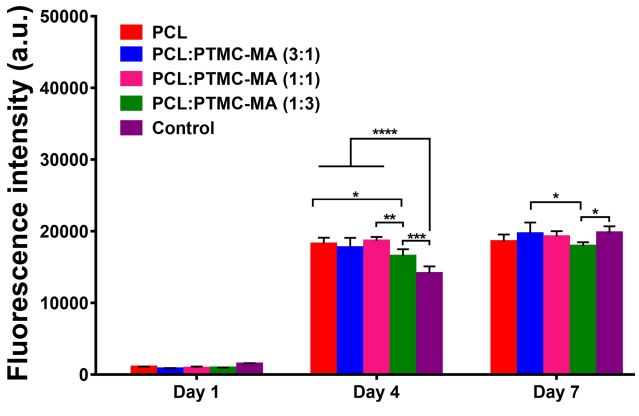

Figure 6 Viability of MSCs on PCL scaffolds and PCL/PTMC-MA composite scaffolds. Tissue culture plates were used as a control. *p< 0.05, ***p< 0.001, and ****p< 0.0001, *p < 0.05 stand for statistical significance.

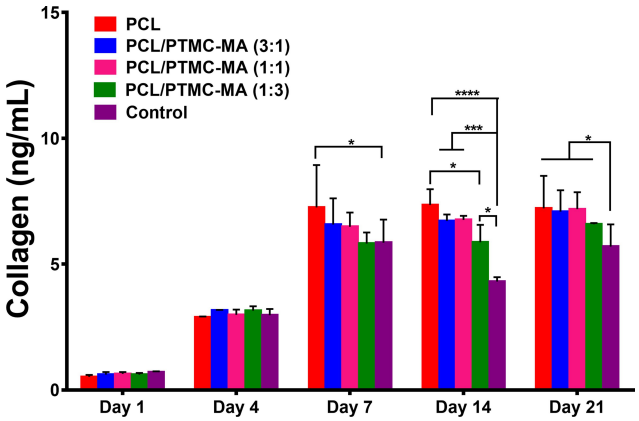

Figure 7 Quantification of collagen I deposited by MSCs on PCL scaffolds and PCL/PTMC-MA composite scaffolds. Tissue culture plates were used as a control. *p< 0.05, ***p< 0.001, and ****p< 0.0001, *p < 0.05 stand for statistical significance.

Conclusions

In the present study, photo-crosslinked PCL/PTMC-MA composite scaffolds were successfully fabricated by electrospinning. The fiber morphology and mechanical properties of PCL/PTMC-MA composite scaffolds were affected by PTMC-MA content. Due to integration of PTMC and formation of crosslinked network, photo-crosslinked PCL/PTMC-MA composite scaffolds showed superior mechanical properties compared to pure PCL scaffolds, including creep resistance, Young's modulus, and max stress at break. Photo-crosslinked PCL/PTMC-MA (1:3) composite scaffolds which had a Young's modulus of 31.13 ± 1.30 MPa and max stress at break of 23.80 ± 3.44 MPa showed comparable mechanical properties with native tendon (Young's modulus 20–1200 MPa, max stress at break 5–100 MPa). Cellular evaluation results demonstrated that PCL/PTMC-MA composite scaffolds were biocompatible for cell adhesion, proliferation, and differentiation. Thus, PCL/PTMC-MA composite scaffold is a promising material for tendon tissue regeneration.

Funding

L.S. appreciates the financial support from the National Natural Science Foundation of China (61574065), the Science and Technology Project of Guangdong Province (2017B020240002), and the Science and Technology Program of Guangzhou (No. 2019050001). H.C. thanks the National Natural Science Foundation of China for financial support (No. 31900976). Y.D. would like to

thank the South China University of Technology for financial support (grant number: x2yx/D6191830).

Disclosure

The authors report no conflicts of interest in this work.

References

1. Laranjeira M, Domingues RMA, Costa-Almeida R, Reis RL, Gomes ME. 3D mimicry of native-tissue-fiber architecture guides tendon-derived cells and adipose stem cells into artificial tendon constructs. *Small*. 2017;13(31):1700689. doi:10.1002/smll.201700689
2. Benjamin M, Kaiser E, Milz S. Structure-function relationships in tendons: a review. *J Anat*. 2008;212(3):211–228. doi:10.1111/j.1469-7580.2008.00864.x
3. Abbah SA, Spanoudes K, O'Brien T, Pandit A, Zeugolis DI. Assessment of stem cell carriers for tendon tissue engineering in pre-clinical models. *Stem Cell Res Ther*. 2014;5(2):1–9. doi:10.1186/scrt426
4. Derwin KA, Baker AR, Spragg RK, Leigh DR, Iannotti JP. Commercial extracellular matrix scaffolds for rotator cuff tendon repair - biomechanical, biochemical, and cellular properties. *J Bone Joint Surg Am*. 2006;88A(12):2665–2672. doi:10.2106/00004623-200612000-00014
5. Calleja M, Connell DA. The achilles tendon. *Semin Musculoskelet Radiol*. 2010;14(3):307–322. doi:10.1055/s-0030-1254520
6. Lomas AJ, Ryan CNM, Sorushanova A, et al. The past, present and future in scaffold-based tendon treatments. *Adv Drug Deliv Rev*. 2015;84:257–277. doi:10.1016/j.addr.2014.11.022
7. Langer R, Vacanti JP. Tissue engineering. *Science*. 1993;260(5110):920–926. doi:10.1126/science.8493529
8. Laurencin CT, Ambrosio AMA, Borden MD, Cooper JA. Tissue engineering: orthopedic applications. *Annu Rev Biomed Eng*. 1999;1(1):19–46. doi:10.1146/annurev.bioeng.1.1.19
9. Spector M. Biomaterials-based tissue engineering and regenerative medicine solutions to musculoskeletal problems. *Swiss Med Wkly*. 2007;137 Suppl 155(Suppl 155):157S–165S.
10. Xu C, Lee W, Dai G, Hong Y. Highly elastic biodegradable single-network hydrogel for cell printing. *ACS Appl Mater Interfaces*. 2018;10(12):9969–9979. doi:10.1021/acsami.8b01294
11. Younesi M, Islam A, Kishore V, Anderson JM, Akkus O. Tenogenic induction of human MSCs by anisotropically aligned collagen biotextiles. *Adv Funct Mater*. 2014;24(36):5762–5770. doi:10.1002/adfm.201400828
12. Cheng S, Jin Y, Wang N, et al. Self-adjusting, polymeric multilayered roll that can keep the shapes of the blood vessel scaffolds during biodegradation. *Adv Mater*. 2017;29(28). doi:10.1002/adma.201700681.
13. Yang G, Li X, He Y, Ma J, Ni G, Zhou S. From nano to micro to macro: electrospun hierarchically structured polymeric fibers for biomedical applications. *Prog Polym Sci*. 2018;81:80–113. doi:10.1016/j.progpolymsci.2017.12.003
14. Bhardwaj N, Kundu SC. Electrospinning: a fascinating fiber fabrication technique. *Biotechnol Adv*. 2010;28(3):325–347. doi:10.1016/j.biotechadv.2010.01.004
15. Sheikh FA, Macossay J, Cantu T, et al. Imaging, spectroscopy, mechanical, alignment and biocompatibility studies of electrospun medical grade polyurethane (Carbothane 3575A) nanofibers and composite nanofibers containing multiwalled carbon nanotubes. *J Mech Behav Biomed Mater*. 2015;41:189–198. doi:10.1016/j.jmbbm.2014.10.012
16. Wu G, Deng X, Song J, Chen F. Enhanced biological properties of biomimetic apatite fabricated polycaprolactone/chitosan nanofibrous bio-composite for tendon and ligament regeneration. *J Photochem Photobiol B*. 2018;178:27–32. doi:10.1016/j.jphotobiol.2017.10.011
17. Tu T, Shen Y, Wang X, et al. Tendon ECM modified bioactive electrospun fibers promote MSC tenogenic differentiation and tendon regeneration. *Appl Mater Today*. 2020;18:100495. doi:10.1016/j.apmt.2019.100495
18. Sharma B, Malik P, Jain P. Biopolymer reinforced nanocomposites: a comprehensive review. *Mater Today Commun*. 2018;16:353–363. doi:10.1016/j.mtcomm.2018.07.004
19. Zant E, Grijpma DW. Synthetic biodegradable hydrogels with excellent mechanical properties and good cell adhesion characteristics obtained by the combinatorial synthesis of photo-cross-linked networks. *Biomacromolecules*. 2016;17(5):1582–1592. doi:10.1021/acs.biomac.5b01721
20. Chen F, Hayami JWS, Amsden BG. Electrospun poly(L-lactide-co-acryloyl carbonate) fiber scaffolds with a mechanically stable crimp structure for ligament tissue engineering. *Biomacromolecules*. 2014;15(5):1593–1601. doi:10.1021/bm401813j
21. Feng J, Zhuo R-X, Zhang X-Z. Construction of functional aliphatic polycarbonates for biomedical applications. *Prog Polym Sci*. 2012;37(2):211–236. doi:10.1016/j.progpolymsci.2011.07.008
22. Laycock B, Nikolic M, Colwell JM, et al. Lifetime prediction of biodegradable polymers. *Prog Polym Sci*. 2017;71:144–189. doi:10.1016/j.progpolymsci.2017.02.004
23. Ren Y, Wei Z, Leng X, Wu T, Bian Y, Li Y. Relationships between architectures and properties of highly branched polymers: the cases of amorphous poly(trimethylene carbonate) and crystalline poly(epsilon-caprolactone). *J Phys Chem B*. 2016;120(17):4078–4090. doi:10.1021/acs.jpcb.6b01867
24. Nitta K, Kimoto A, Watanabe J. Surface properties of amphiphilic graft copolymer containing different oligo segments. *Polymer*. 2016;96:45–53. doi:10.1016/j.polymer.2016.04.055
25. Mi H-Y, Jing X, Yu E, Wang X, Li Q, Turng L-S. Manipulating the structure and mechanical properties of thermoplastic polyurethane/polycaprolactone hybrid small diameter vascular scaffolds fabricated via electrospinning using an assembled rotating collector. *J Mech Behav Biomed Mater*. 2018;78:433–441. doi:10.1016/j.jmbbm.2017.11.046
26. Yang L, Li J, Li M, Gu Z. The in vitro and in vivo degradation of cross-linked poly(trimethylene carbonate)-based networks. *Polymers*. 2016;8(4):151. doi:10.3390/polym8040151
27. Yang L, Li J, Meng S, et al. The in vitro and in vivo degradation behavior of poly (trimethylene carbonate-co-epsilon-caprolactone) implants. *Polymer*. 2014;55(20):5111–5124. doi:10.1016/j.polymer.2014.08.027
28. Guo Z, Grijpma DW, Poot AA. Preparation and characterization of flexible and elastic porous tubular PTMC scaffolds for vascular tissue engineering. *Polym Adv Technol*. 2017;28(10):1239–1244. doi:10.1002/pat.3954
29. Tao J, Guoquan Z, Hui L, Xun J. Preparation of electrospun poly (epsilon-caprolactone)/poly (trimethylene-carbonate) blend scaffold for in situ vascular tissue engineering. *Adv Mat Res*. 2013;629:60–63.
30. Dienel KEG, van Bochove B, Seppala JV. Additive manufacturing of bioactive poly(trimethylene carbonate)/β-tricalcium phosphate composites for bone regeneration. *Biomacromolecules*. 2020;21(2):366–376. doi:10.1021/acs.biomac.9b01272
31. Guillaume O, Geven MA, Sprecher CM, et al. Surface-enrichment with hydroxyapatite nanoparticles in stereolithography-fabricated composite polymer scaffolds promotes bone repair. *Acta Biomater*. 2017;54:386–398. doi:10.1016/j.actbio.2017.03.006
32. Zhang Y, Liang R-J, Xu -J-J, et al. Efficient induction of antimicrobial activity with vancomycin nanoparticle-loaded poly(trimethylene carbonate) localized drug delivery system. *Int J Nanomed*. 2017;12:1201–1214. doi:10.2147/IJN.S127715
33. Zhang X, Geven MA, Wang X, et al. A drug eluting poly(trimethylene carbonate)/poly(lactic acid)-reinforced nanocomposite for the functional delivery of osteogenic molecules. *Int J Nanomedicine*. 2018;13:5701–5718. doi:10.2147/IJN.S163219

34. Trinca RB, Abraham GA, Felisberti MI. Electrospun nanofibrous scaffolds of segmented polyurethanes based on PEG, PLLA and PTMC blocks: physico-chemical properties and morphology. *Mater Sci Eng C-Mater Biol Appl*. 2015;56:511–517. doi:10.1016/j.msec.2015.07.018
35. Song Y, Yang F, Jansen JA, et al. Poly(trimethylene carbonate) porous tubular structures made by electro-spinning. *J Control Release*. 2008;132(3):79–80. doi:10.1016/j.jconrel.2008.09.071
36. Geven MA, Barbieri D, Yuan H, de Bruijn JD, Grijpma DW. Preparation and mechanical properties of photo-crosslinked poly(trimethylene carbonate) and nano-hydroxyapatite composites. *Clin Hemorheol Microcirc*. 2015;60(1):3–11. doi:10.3233/CH-151936
37. Jimenez-Pardo I, van der Ven LGJ, van Benthem RATM, Esteves ACC, de With G. Effect of a set of acids and polymerization conditions on the architecture of polycarbonates obtained via ring opening polymerization. *J Polym Sci a Polym Chem*. 2017;55(9):1502–1511.
38. Sun J, Jung D, Schoppa T, et al. Light-responsive serinol-based polycarbonate and polyester as degradable scaffolds. *ACS Appl Bio Mater*. 2019;2(7):3038–3051. doi:10.1021/acsabm.9b00347
39. Cristofaro F, Gigli M, Bloise N, et al. Influence of the nanofiber chemistry and orientation of biodegradable poly(butylene succinate)-based scaffolds on osteoblast differentiation for bone tissue regeneration. *Nanoscale*. 2018;10(18):8689–8703. doi:10.1039/C8NR00677F
40. Cardwell RD, Dahlgren LA, Goldstein AS. Electrospun fibre diameter, not alignment, affects mesenchymal stem cell differentiation into the tendon/ligament lineage. *J Tissue Eng Regen Med*. 2014;8(12):937–945. doi:10.1002/term.1589
41. Mouw JK, Ou G, Weaver VM. Extracellular matrix assembly: a multiscale deconstruction. *Nat Rev Mol Cell Biol*. 2014;15(12):771–785. doi:10.1038/nrm3902
42. Li X, Yin H-M, Su K, et al. Polydopamine-assisted anchor of chitosan onto porous composite scaffolds for accelerating bone regeneration. *ACS Biomater Sci Eng*. 2019;5(6):2998–3006. doi:10.1021/acsbiomaterials.9b00209
43. Wang X, Zhao H, Turng L-S LQ. Crystalline morphology of electrospun poly(ε-caprolactone) (PCL) nanofibers. *Ind Eng Chem Res*. 2013;52(13):4939–4949. doi:10.1021/ie302185e
44. Fadaie M, Mirzaei E, Geramizadeh B, Asvar Z. Incorporation of nanofibrillated chitosan into electrospun PCL nanofibers makes scaffolds with enhanced mechanical and biological properties. *Carbohydr Polym*. 2018;199:628–640. doi:10.1016/j.carbpol.2018.07.061
45. Ekram B, Abd El-Hady BM, El-Kady AM, et al. Enhancing the stability, hydrophilicity, mechanical and biological properties of electrospun polycaprolactone in formic acid/acetic acid solvent system. *Fibers Polym*. 2019;20(4):715–724. doi:10.1007/s12221-019-8795-1
46. Wang Z, Liang R, Jiang X, et al. Electrospun PLGA/PCL/OCP nanofiber membranes promote osteogenic differentiation of mesenchymal stem cells (MSCs). *Mater Sci Eng C-Mater Biol Appl*. 2019;104:109796. doi:10.1016/j.msec.2019.109796
47. Zhao Q, Wang J, Cui H, Chen H, Wang Y, Du X. Programmed shape-morphing scaffolds enabling facile 3D endothelialization. *Adv Funct Mater*. 2018;28(29):1801027. doi:10.1002/adfm.201801027
48. Tiwari AP, Joshi MK, Park CH, Kim CS. Nano-nets covered composite nanofibers with enhanced biocompatibility and mechanical properties for bone tissue engineering. *J Nanosci Nanotechnol*. 2018;18(1):529–537. doi:10.1166/jnn.2018.13930
49. Silva JC, Udangawa RN, Chen JL, et al. Kartogenin-loaded coaxial PGS/PCL aligned nanofibers for cartilage tissue engineering. *Mater Sci Eng C-Mater Biol Appl*. 2020;107:110291. doi:10.1016/j.msec.2019.110291
50. LaCroix AS, Duenwald-Kuehl SE, Lakes RS, Vanderby R Jr. Relationship between tendon stiffness and failure: a metaanalysis. *J Appl Physiol*. 2013;115(1):43–51. doi:10.1152/japplphysiol.01449.2012
51. Chen Y, Yu B, Xue G, et al. Effects of storage solutions on the viability of human umbilical cord mesenchymal stem cells for transplantation. *Cell Transplant*. 2013;22(6):1075–1086. doi:10.3727/096368912X657602
52. Kleinman HK, Klebe RJ, Martin GR. Role of collagenous matrices in the adhesion and growth of cells. *J Cell Biol*. 1981;88(3):473–485. doi:10.1083/jcb.88.3.473